

An Experimental Charge Density Study of the Effect of the Noncentric Crystal Field on the Molecular Properties of Organic NLO Materials**

R. Srinivasa Gopalan,^[a] Giridhar U. Kulkarni,^[a] and C. N. R. Rao^{*[a]}

The structure, packing, and charge distribution in molecules of nonlinear optical materials have been analysed with reference to their counterparts in centrosymmetric structures based on low temperature X-ray measurements. The systems studied are the centric and noncentric polymorphs of 5-nitrouracil as well as the diamino, dithio, and thioamino derivatives of 1,1-ethylenedicarbonitrile; the latter possesses a noncentric structure. The molecular structure of 5-nitrouracil is invariant between the two forms, while the crystal packing is considerably different, leading to dimeric N–H...O rings in the centric polymorph and linear chains in noncentric one. There is an additional C–H...O contact in the centric form with a significant overlap of the electrostatic potentials between the alkenyl hydrogen atom and an oxygen atom of the nitro group. The dipole moment of 5-nitrouracil in the noncentric form is much higher ($\mu = 9$ D) than in the centric form (≈ 6 D). Among the 1,1-ethylenedicarbonitriles, there is an increased charge separation in the noncentric thioamino derivative,

leading to an enhanced dipole of 15 D compared to the centric diamino (5 D) and dithio (6 D) derivatives. The effect of the crystal field is borne out by semiempirical AM1 calculations on the two systems. Dipole moments calculated for the molecules in the frozen geometries match closely with those obtained for centric crystals from the experimental charge densities. The calculated values of the dipole moment in the frozen or optimized geometries in the noncentric structures are, however, considerably lower than the observed value. Furthermore, the conformation of the S–CH₃ group in the noncentric crystal is anti with respect to the central C=C bond while the syn conformation is predicted for the free molecule in the optimized geometry.

KEYWORDS:

charge density · dipole moment · materials science · nonlinear optics · semiempirical calculations

Several organic materials with nonlinear optical (NLO) properties have been described in the recent literature.^[1–5] Nitroaniline and push–pull ethylenes are typical examples of NLO materials involving intramolecular charge transfer. Besides having a polarizable π -cloud with electron-donating and -accepting groups, an essential feature of such compounds is that they crystallize in noncentrosymmetric space groups. Espinosa et al.^[6] have reported a charge density study of L-arginine phosphate. Puig-Molina et al.^[7] have compared the topological properties of charge density of 2-amino-5-nitropyridinium dihydrogen phosphate from experiment and theory. Charge density studies of 2-methyl-4-nitroaniline^[8] and urea^[9] show that there is a considerable enhancement of the molecular dipole moment in the solid state. Based on a charge density study on *N*-(4-nitrophenyl)-L-prolinol, Fkyerat et al.^[10, 11] extracted hyperpolarizability from the octapole moments. Such a possibility has been discussed in connection with inorganic NLO materials as well.^[12, 13] While there is some speculation as to whether charge densities can provide hyperpolarizability,^[14] it is generally accepted that reliable molecular dipole moments can be extracted from charge densities.^[15] Thus, Hamzaoui et al.^[16] obtained the dipole moment of 3-methyl-4-nitropyridine-*N*-oxide from its charge density, which agrees well with that from semiempirical calculations. Recently, Madsen et al.^[17] have evaluated the dipole moment of phosphogulene from its charge

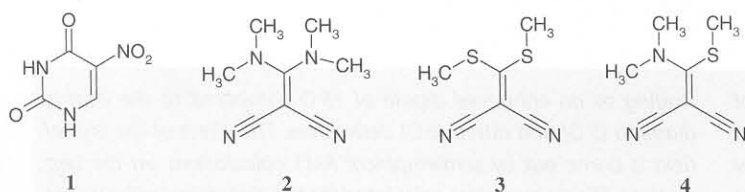
density to be 42% higher than that measured in a chloroform solution. They also obtained the pyroelectric coefficient by combining the derived dipole moment with temperature-dependent measurements of the unit cell volume.

We have carried out an experimental charge density investigation of organic NLO systems in order to understand the manner in which the noncentric nature of the crystal field affects the molecular dipole moment and other properties in the solid. For this purpose, we have examined two systems—one where the center of symmetry is destroyed by crystallizing the molecule in a related polymorphic structure and the other where the noncentric nature is introduced by changing the pattern of substitution. For the first system, we have chosen the two polymorphic forms of 5-nitrouracil, **1**, which crystallizes in orthorhombic *P*₂₁₂₁ and *Pbca* space groups, the former being noncentrosymmetric. The NLO activity of the noncentric form at 1.06 μ m is ~ 160 times that of potassium dihydrogen phos-

[a] Prof. Dr. C. N. R. Rao, R. S. Gopalan, Dr. G. U. Kulkarni
Chemistry and Physics of Materials Unit
Jawaharlal Nehru Centre for Advanced Scientific Research
Jakkur P.O., Bangalore, 560064 (India)
E-mail: cnrrao@jncasr.ac.in

[**] The authors thank Dr. S. N. Ghanshyam Acharya for the synthesis of dicarbonitrile derivatives 2–4.

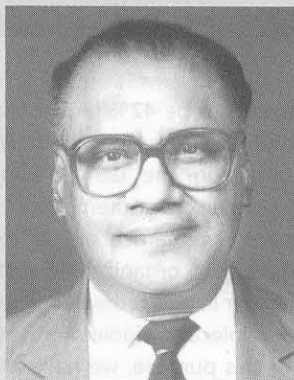
phate.^[18] In order to explore the effect of substitution, we have studied 1,1-ethylenedicarbonitriles (EDCN), in which the positions of the dimethylamino and methylthio substituents have been varied to give the symmetric and unsymmetric molecules bis(*N,N*-dimethylamino)-EDCN (**2**), 2,2-bis(methylthio)-EDCN (**3**), and 2-(*N,N*-dimethylamino)-2-methylthio-EDCN (**4**). The diamino and the dithio derivatives, **2** and **3**, crystallize in centric



structures whereas the thioamino, **4**, occurs in a noncentrosymmetric structure exhibiting NLO properties. In both the systems, we have examined the intramolecular bonding using the Laplacian of the total electron density. Where necessary, we have analyzed the intermolecular interactions in terms of the electrostatic potential. We have computed the dipole moments from the experimental charge densities and compared the results with those from semiempirical AM1 calculations.

Editorial Advisory Board Member: * C. N. R. Rao

received his M.Sc. in Chemistry from Banaras Hindu University (1953), Ph.D. in Chemistry from Purdue University (1958), and D.Sc. from the University of Mysore (1961). Following post-doctoral study in Berkeley, he worked as a faculty member at the Indian Institute of Technology, Kanpur, and the Indian Institute of Science, Bangalore. His main research interests are in the chemistry of materials and chemical spectroscopy. He is at present the Linus Pauling Research Professor at the JNCASR. He has been a Visiting Professor at the Universities of Cardiff, Cambridge, and California at Santa Barbara. He is a member of the Royal Society, US National Academy of Sciences, Pontifical Academy of Sciences, French Academy of Sciences, Japan Academy, and several others. He is a recipient of the Marlow Medal of the Faraday Society, Einstein Medal of UNESCO, Centenary Medal of the Royal Society of Chemistry, and the Hughes Medal of the Royal Society.



[*] Members of the Editorial Advisory Board will be introduced to the readers with their first manuscript.

5-Nitrouracil

The centric polymorph of **1** crystallizes with eight molecules per unit cell (*Pbca*; $a = 8.308(3)$, $b = 10.426(3)$, $c = 13.363(4)$ Å) while the unit cell of the noncentric form contains four molecules (*P2₁2₁2₁*; $a = 5.4342(1)$, $b = 9.8406(1)$, $c = 10.3659(1)$ Å). The densities of both forms are similar (Table 1).

The space groups *Pbca* and *P2₁2₁2₁* contain the same set of symmetry elements but for the inversion center, which makes the problem interesting. In both polymorphs, the asymmetric unit comprises a whole molecule. The intramolecular geometry is essentially the same in both cases and the molecule is nearly planar (Table 2): The nitro group forms an angle of 1.5° with the plane of the uracil ring in the centric form and 2.0° in the noncentric polymorph.

In Figure 1, the packing diagram along with the atom labels are shown. In the centric form, the molecule is held by the dimeric N–H...O contacts of $R_2^2(8)$ type^[19] with the two neighboring coplanar molecules (Figure 1a). The N–H...O contacts in the noncentric form are of $D(2)$ type arising from four different molecules (Figure 1b). In both the cases, the N–H...O bonds are ~1.8 Å long, with \angle N–H...O angles of 155–174°. The centric polymorph, in addition, exhibits an intermolecular C–H...O interaction with the nitro group at a relatively short distance of 2.15 Å. The nitro group of the noncentric polymorph is in an unfavorable geometry to establish such a contact (Figure 1b).

The results of the multipolar refinement (see Experimental Section) are described using the Laplacian of the total charge density. The topology of the Laplacian field allows one to obtain a chemical model of the bonded and nonbonded pairs and to characterize the local concentration ($\nabla^2\rho < 0$) and depletion ($\nabla^2\rho > 0$) of the molecular charge distribution.^[20, 21] Figure 2 shows the contour maps of the negative Laplacian obtained for the two polymorphs. The lone electron pairs on the oxygen

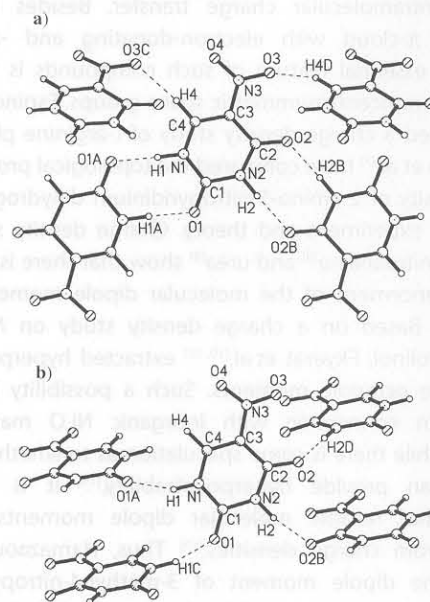


Figure 1. Molecular packing in a) centric and b) noncentric **1** showing the intermolecular hydrogen bonds. Atom labels are also shown.

Table 1. Crystal data for 5-nitrouracil (1) and the 1,1-ethylenedicarbonitriles (2–4).^[a]

Crystal	1		2	3	4
	centric	noncentric			
Chemical formula (g mol ⁻¹)	C ₄ H ₃ N ₃ O ₄ (157.09)		C ₈ H ₁₂ N ₄ (164.22)	C ₈ H ₈ N ₂ S ₂ (170.25)	C ₇ H ₉ N ₃ S (167.23)
Crystal system	orthorhombic	orthorhombic	orthorhombic	monoclinic	orthorhombic
Space group	<i>Pbca</i> (No. 61)	<i>P2₁2₁2₁</i> (No. 19)	<i>Pcab</i> (No. 6)	<i>P2₁/n</i> (No. 14)	<i>Pna2₁</i> (No. 33)
<i>a</i> [Å]	8.308(3)	5.4342(1)	7.6280(1)	4.0261(1)	7.904(2)
<i>b</i> [Å]	10.426(3)	9.8406(1)	14.455	13.227	8.630(2)
<i>c</i> [Å]	13.363(4)	10.3659(1)	16.3489(2)	14.3906(1)	12.856(3)
β [°]	90	90	90	95.445(1)	90
<i>V</i> [cm ³]	1157.5(6)	554.32(1)	1802.70(3)	762.89(2)	876.9(3)
<i>Z</i>	8	4	8	4	4
<i>F</i> ₀₀₀	640	320	704	352	352
ρ [g cm ⁻³]	1.803	1.882	1.210	1.482	1.267
No. of reflections for cell parameters	45	37	60	60	60
μ [mm ⁻¹]	0.16	0.17	0.079	0.617	0.309
Crystal form	cuboidal	hexagonal	cuboidal	cuboidal	cuboidal
Crystal size [mm]	0.3 × 0.2 × 0.2	0.15 × 0.15 × 0.1	0.2 × 0.1 × 0.1	0.2 × 0.15 × 0.1	0.2 × 0.1 × 0.1
Crystal color	colorless	colorless	colorless	yellow	colorless
No. of measured reflections	16262	16515	29153	12914	24387
No. of independent reflections	5026	8371	8589	6451	8576
No. of observed reflections	3879	3239	4894	4863	2874
<i>R</i> _{merge}	0.0644	0.0434			
<i>R</i> _{int}	0.0763	0.0454	0.0361	0.0301	0.0692
θ _{min} [°]	3.0	2.8	2.49	2.10	2.84
θ _{max} [°]	49.4	49.4	49.48	49.47	49.89
Range of <i>h</i> , <i>k</i> , <i>l</i>	–12 ≤ <i>h</i> ≤ 16 –22 ≤ <i>k</i> ≤ 11 –28 ≤ <i>l</i> ≤ 27	–10 ≤ <i>h</i> ≤ 11 –19 ≤ <i>k</i> ≤ 20 –21 ≤ <i>l</i> ≤ 21	–15 ≤ <i>h</i> ≤ 15 –15 ≤ <i>k</i> ≤ 30 –34 ≤ <i>l</i> ≤ 34	–8 ≤ <i>h</i> ≤ 7 –21 ≤ <i>k</i> ≤ 27 –29 ≤ <i>l</i> ≤ 28	–16 ≤ <i>h</i> ≤ 15 –18 ≤ <i>k</i> ≤ 18 –27 ≤ <i>l</i> ≤ 27
After multipole refinement					
Weighting scheme	0.02, 0.3	0.02, 0.1	0.05, 0.5	0.03, 0.3	0.04, 0.3
<i>R</i> ₁	0.0345	0.0391	0.0501	0.0397	0.0332
<i>wR</i> ₂	0.0416	0.0454	0.0775	0.0475	0.0513
<i>S</i>	1.05	1.00	0.94	1.06	1.27
No. of variables	399	404	161	178	197
<i>N</i> _{ref} / <i>N</i> _v	20.5	17.2	30.4	27.3	14.6
Cambridge Crystallographic Database	145990	145991	145987	145988	145989

[a] Experimental details: Siemens CCD diffractometer, crystal–detector distance 5.0 cm, Mo_{K α} radiation ($\lambda = 0.71073$ Å, 50 kV, 40 mA), 130 ± 1 K

atoms occur as (3, –3) critical points. There are some differences in the Laplacian maps of the two polymorphs. The atomic basins are generally linked in the centrosymmetric form but they appear to be disjoint in the noncentric case. The N3–O3 bond region in the centrosymmetric form contains nonoverlapping atomic lobes, which indicate a closed shell interaction. This is reflected in the properties of the bond critical points, listed in Table 3. This bond carries a much smaller Laplacian ($-3.0 \text{ e} \text{ \AA}^{-5}$) compared to the other N–O bond of the molecule as well as the N–O bonds of the noncentric form, though the electron density itself is quite comparable. We also notice from Table 3 that the densities and the associated Laplacians of the non-hydrogen bonds are somewhat higher in the noncentric form while those of the N–H bonds are higher in the centric form. Moreover, the pseudo-atomic charges are generally higher in the noncentric polymorph. This implies that there is an increased charge separation in the noncentric case. The nitro group charge is -0.19 and -0.38 e respectively, in the centric and the noncentric forms, which compare well with -0.25 e obtained for 3-methyl-4-nitropyridine-*N*-oxide.^[16] We also observe that the properties of the various bonds of the uracil moiety match closely with those reported in the case of 1-methyluracil.^[22]

The nature of the intermolecular bonding is described in terms of the electrostatic potential. In Figure 3, contour maps of the electrostatic potential maps in the N–H...O and the C–H...O bond regions are shown. The contours originating from the N–H region overlap with those from the oxygen atom (Figures 3a, b). The penetration is significant and indicates that these are strong contacts.^[23] They are associated with (3, –1) critical points in ρ as well as in electrostatic potential. The Laplacian at the CPs are small and positive (Table 4), as generally found in hydrogen bonds.^[24] The C–H...O contact of the centric form also exhibits a noticeable overlap of the potentials ($\rho = 0.08(2) \text{ e} \text{ \AA}^{-3}$, $V = 0.28(1) \text{ e} \text{ \AA}^{-1}$), while in the noncentric form a zero potential surface passes between the proton and the oxygen atom to indicate no interaction between them (Figure 3c). This is understandable, since in the presence of a carbonyl group, a nitro group acts as a secondary hydrogen bond acceptor.^[25] The C–H...O contact of the centric form is special in that the oxygen O3, which participates in intermolecular bonding, tends to have nearly ionic interaction with the nitro group (Figure 2). Such bonding would be favored by the centrosymmetric packing of the molecules. For the same reason, this contact is absent in the noncentric form.

Table 2. Bond lengths and angles of 1.

Bond length [Å]	centric 1	noncentric 1
O1-C1	1.2284(13)	1.2310(13)
O2-C2	1.2252(13)	1.2290(12)
O4-N3	1.2364(12)	1.235(2)
O3-N3	1.2294(12)	1.2306(14)
N2-C1	1.3667(13)	1.3663(12)
N2-C2	1.3945(13)	1.3900(14)
N2-H2	1.01	1.01
N1-C4	1.3427(14)	1.341(2)
N1-C1	1.3807(13)	1.3786(14)
N1-H1	1.01	1.01
N3-C3	1.4432(13)	1.4412(14)
C2-C3	1.4568(14)	1.454(2)
C3-C4	1.3575(14)	1.3621(14)
C4-H4	1.08	1.08
Bond angle [°]	centric 1	noncentric 1
C1-N2-C2	127.18(9)	127.47(9)
C1-N2-H2	116.41(6)	116.27(6)
C2-N2-H2	116.41(6)	116.27(6)
C4-N1-C1	122.51(9)	122.90(8)
C4-N1-H1	118.74(6)	118.55(6)
C1-N1-H1	118.74(6)	118.55(5)
O3-N3-O4	123.09(9)	123.46(11)
O3-N3-C3	119.36(9)	119.20(11)
O4-N3-C3	117.56(9)	117.33(10)
O1-C1-N2	123.08(9)	122.60(10)
O1-C1-N1	121.61(9)	122.54(9)
N2-C1-N1	115.31(9)	114.85(9)
O2-C2-N2	119.86(9)	118.82(10)
O2-C2-C3	127.55(10)	128.32(10)
N2-C2-C3	112.59(8)	112.85(8)
C4-C3-N3	116.49(9)	116.94(10)
C4-C3-C2	120.79(9)	120.32(10)
N3-C3-C2	122.62(8)	122.73(9)
N1-C4-C3	121.39(9)	121.40(10)
N1-C4-H4	119.30(6)	119.30(6)
C3-C4-H4	119.30(6)	119.30(7)

In situ dipole moments of molecules in crystals can be obtained from charge densities by using Equation (1).

$$\mu_i = \sum_j z_j R_i + \int r_i \rho_i(r_i) dr \quad (1)$$

The XDPROP routine (the XD program) was used to calculate dipole moments and the dipole moment vectors are shown in Figure 4. The vectors lie close to the N(1)–H(1) bond direction in the plane of the molecule, with magnitudes of $\mu = 5.5(6)$ and $9(1)$ D in the centric and the noncentric polymorphs, respectively.^[26] As the intramolecular geometry remains the same in the two cases (Table 2), the enhancement of the dipole moment in the noncentric structure is likely to arise mainly due to packing. The effect of crystal packing can be understood by calculating the dipole moment of the molecule *ex situ* in the frozen geometry. For this purpose, we carried out AM1, PRECISE calculations by freezing the molecular geometries obtained from X-ray diffraction. The calculated dipole moments are very similar in the two polymorphs ($\mu = 5.5$ and 5.6 D for centric and noncentric cases, respectively) and point in the same direction (Figure 4). Interestingly, the vectors obtained from the calculation lie close (in magnitude as well as in direction) to that from

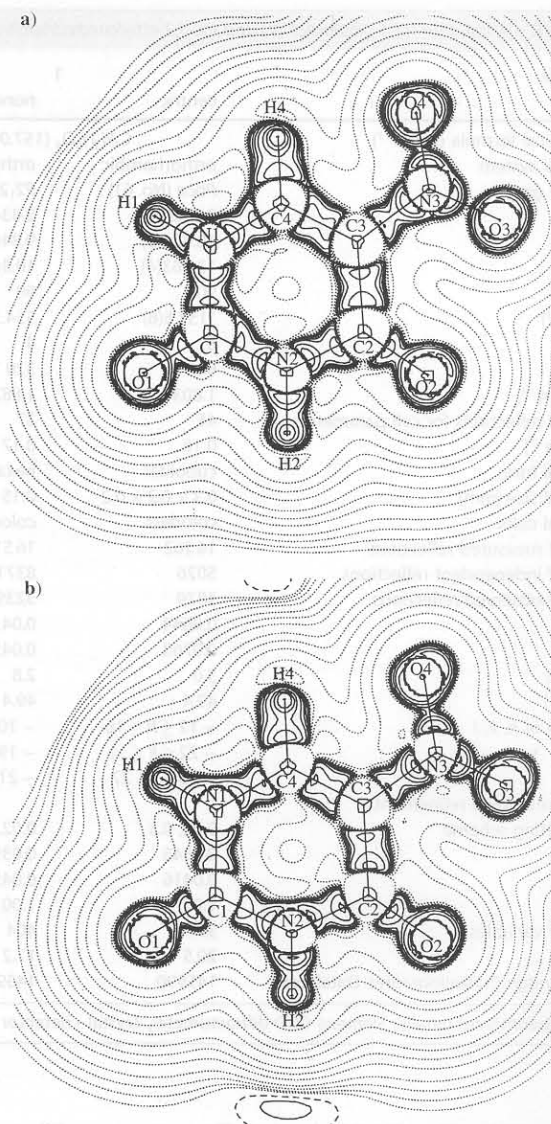


Figure 2. Contour maps of the total density Laplacian in the C1-C2-C4 plane for a) centric and b) noncentric 1.

Table 3. Analysis of the bond critical points in 1.

Bond	centric			noncentric		
	$\rho^{[a]}$	$\nabla^2 \rho^{[b]}$	$\epsilon^{[c]}$	$\rho^{[a]}$	$\nabla^2 \rho^{[b]}$	$\epsilon^{[c]}$
O1-C1	2.91(5)	-38.2(3)	0.21	3.31(9)	-51.9(5)	0.27
O2-C2	2.77(6)	-26.8(4)	0.18	3.21(97)	-51.3(4)	0.17
N1-C1	2.16(5)	-26.8(2)	0.06	2.36(8)	-27.9(3)	0.29
N1-C4	2.29(5)	-27.3(2)	0.25	2.50(9)	-31.5(4)	0.28
N1-H1	1.98(6)	-28.8(4)	0.06	1.9(1)	-30.1(8)	0.00
N2-C1	2.12(4)	-23.9(2)	0.21	2.34(8)	-30.1(3)	0.38
N2-C2	2.09(4)	-23.5(2)	0.12	2.22(7)	-23.7(3)	0.24
N2-H2	1.92(6)	-29.8(4)	0.04	1.8(1)	-36(1)	0.04
N3-C3	1.87(4)	-15.4(2)	0.37	1.96(8)	-17.1(4)	0.39
C2-C3	1.93(3)	-16.0(1)	0.27	1.98(7)	-7.0(2)	0.46
C3-C4	2.21(3)	-22.1(1)	0.34	2.31(7)	-24.7(2)	0.43
C4-H4	1.79(5)	-20.1(2)	0.05	1.9(1)	-29.5(7)	0.07
O3-N3	3.19(5)	-3.0(2)	0.09	3.48(9)	-14.5(3)	0.05
O4-N3	3.28(5)	-11.9(2)	0.08	3.61(9)	-18.6(4)	0.08

[a] electron density, in $e \text{ \AA}^{-3}$. [b] Laplacian, in $e \text{ \AA}^{-5}$. [c] Ellipticity.

Table 4. Hydrogen bond critical points in **1**.

Polymorph	D-H...A	ρ [e Å ⁻³]	$\nabla^2\rho$ [e Å ⁻⁵]	V [e Å ⁻¹]
centric	N(1)-H(1)...O(1) ^[a]	0.18(3)	3.32(2)	0.55(2)
	N(2)-H(2)...O(2) ^[a]	0.17(3)	2.88(2)	0.47(2)
	C(4)-H(4)...O(3) ^[b]	0.08(2)	1.39(1)	0.28(1)
noncentric	N(1)-H(1)...O(1) ^[c]	0.16(5)	2.99(4)	0.52(3)
	N(2)-H(2)...O(2) ^[d]	0.15(6)	3.05(5)	0.61(4)
	O(1)...H(1)-N(1) ^[e]	0.14(5)	2.64(5)	0.53(3)
	O(2)...H(2)-N(2) ^[f]	0.13(5)	2.69(5)	0.60(3)

Symmetries: [a] $-x, -y, 1-z$. [b] $1/2-x, 1/2+y, z$. [c] $1/2+x, 1/2-y, 1-z$. [d] $-1/2+x, 1/2-y, -z$; [e] $-1/2+x, 1/2-y, 1-z$. [f] $1/2+x, 1/2-y, -z$.

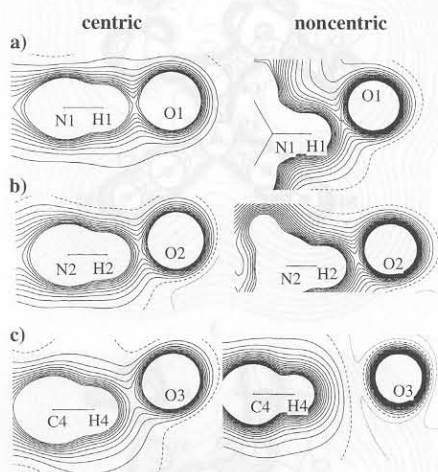


Figure 3. Contour maps of the electrostatic potential in the intermolecular regions (contour level at 0.05 eÅ^{-1}): a) N1-H1...O1, b) N2-H2...O2, c) C4-H4...O3. The centric and noncentric forms are given on the left and right sides, respectively.

experiment for the centric polymorph. This seems to suggest that the packing in the centric form of **1** has a minimal effect on the intramolecular charge distribution. This observation also

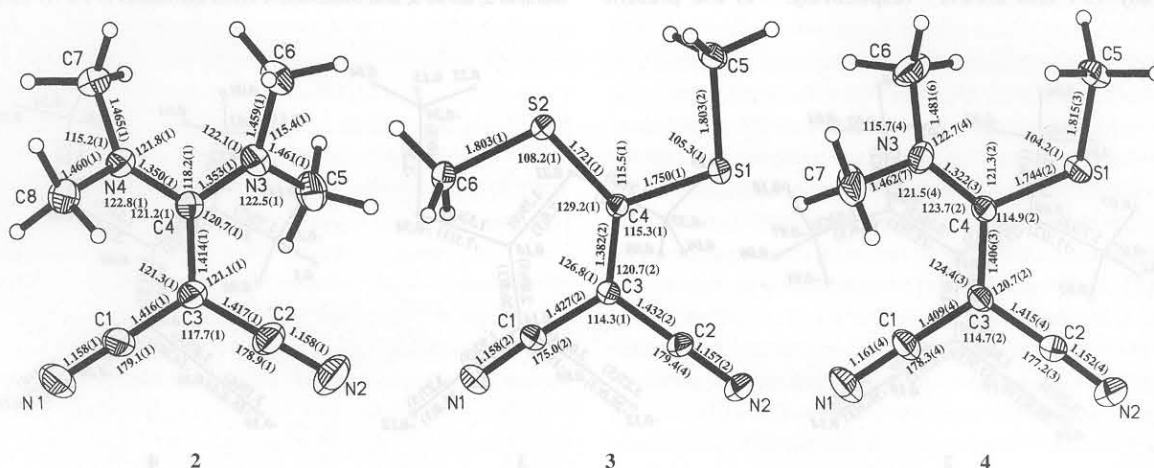


Figure 5. Molecular diagrams of the diamino **2**, dithio **3**, and thioamino **4** EDCN derivatives, showing thermal ellipsoids. The bond lengths and angles of the non-hydrogen bonds are shown.

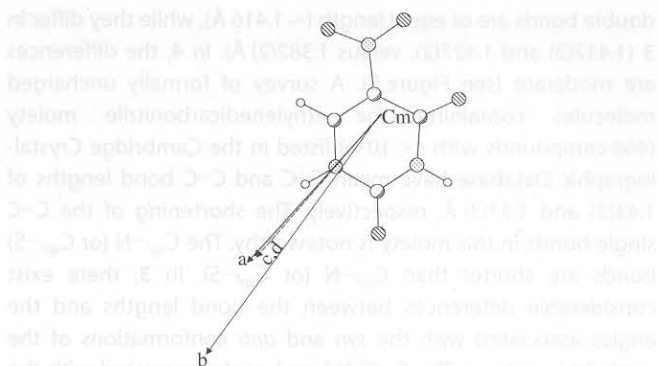


Figure 4. Orientation of the molecular dipole moment of **1**: a) centric, multipole; b) noncentric, multipole; c) centric, AM1; d) noncentric, AM1. Cm refers to the center of mass of the molecule.

demonstrates that an asymmetric crystal field in a noncentric structure can significantly enhance the dipole moment of a molecule. To our knowledge, this is the first instance of charge density study of a compound crystallizing in closely related space groups exhibiting differing molecular properties.

1,1-Ethylenedicarbonitriles

The two nitriles, **2** and **3**, crystallize in the centrosymmetric *Pcab* and *P2₁/n* space groups, respectively, whereas **4** crystallizes in the noncentric *Pna2₁* space group (Table 1). We show the molecular diagrams along with the thermal ellipsoids in Figure 5, where the bond lengths and angles associated with the non-hydrogen atoms are also indicated. Diamine **2** possesses a pseudo two-fold symmetry along C3-C4 while the dithio **3** exhibits a *syn-anti* methylthio conformation. Thioamine **4** has methylthio group in the *anti* conformation. The 1,1-ethylenedicarbonitrile moiety, which contains a formal C3=C4 bond and two single C1-C3 and C2-C3 bonds, along with the cyano group, is essentially planar in all three molecules. The C=N bond lengths are also similar (1.14(3) Å) and close to those reported in the literature. There are however, some differences between the formal C-C single and double bonds. In **2**, the single and the

double bonds are of equal length (~ 1.416 Å), while they differ in **3** (1.432(2) and 1.427(2), versus 1.382(2) Å). In **4**, the differences are moderate (see Figure 5). A survey of formally uncharged molecules containing the ethylenedicarbonitrile moiety (466 compounds with $r < 10\%$) listed in the Cambridge Crystallographic Database have mean C–C and C=C bond lengths of 1.43(2) and 1.37(3) Å, respectively. The shortening of the C–C single bonds in this moiety is noteworthy. The C_{sp^2} –N (or C_{sp^2} –S) bonds are shorter than C_{sp^3} –N (or C_{sp^3} –S). In **3**, there exist considerable differences between the bond lengths and the angles associated with the *syn* and *anti* conformations of the methylthio groups. The C–C≡N bond angle associated with the *syn*-methylthio group is 175° instead of $\sim 180^\circ$. An earlier structural report on this molecule suggested steric interaction to be responsible for the discrepancy.^[27] However, 3,3-bis(methylthio)-2-nitro-2-propene-1-nitrile does not show significant differences in the bond lengths and angles between the *syn*- and the *anti*-configurations of the methylthio groups.^[28]

Figure 6 shows the contour maps of the negative Laplacian of the total density in the plane defined by the N1–N2–C3 atoms. The lone pairs on the nitrogen and sulfur atoms exhibit (3, –3) as critical points. The lobes near sulfur are similar to those seen previously by Mallinson and co-workers in the case of 3,3,6,6-tetramethyl-5-tetrathiane.^[29] In the diamino **2**, the contours associated with the amino groups are small, since this group is out of plane with the rest of the molecule. The C–S bonds of both **3** and **4** exhibit disjoint lobes.

Figure 7 depicts the critical points in the total density for the various bonds in the molecules. The values of total electron density, the Laplacian, and the ellipticity at the critical points are also shown. The C≡N group exhibits similar densities (~ 3.2 eÅ⁻³) in the three molecules although the Laplacian values are somewhat different, –36, –20, and –16 eÅ⁻⁵ in **1**, **2**, and **3**, respectively. Interestingly, the densities of the C–C single and double bonds are not significantly different in the three compounds. The Laplacian values are also similar, the differences are less than ~ 5 eÅ⁻⁵. This result is in contrast with what is expected of normal single and double bonds. The electron densities associated with the isolated single and double bonds are generally 1.71 and 2.5 eÅ⁻³ respectively.^[30] In the present

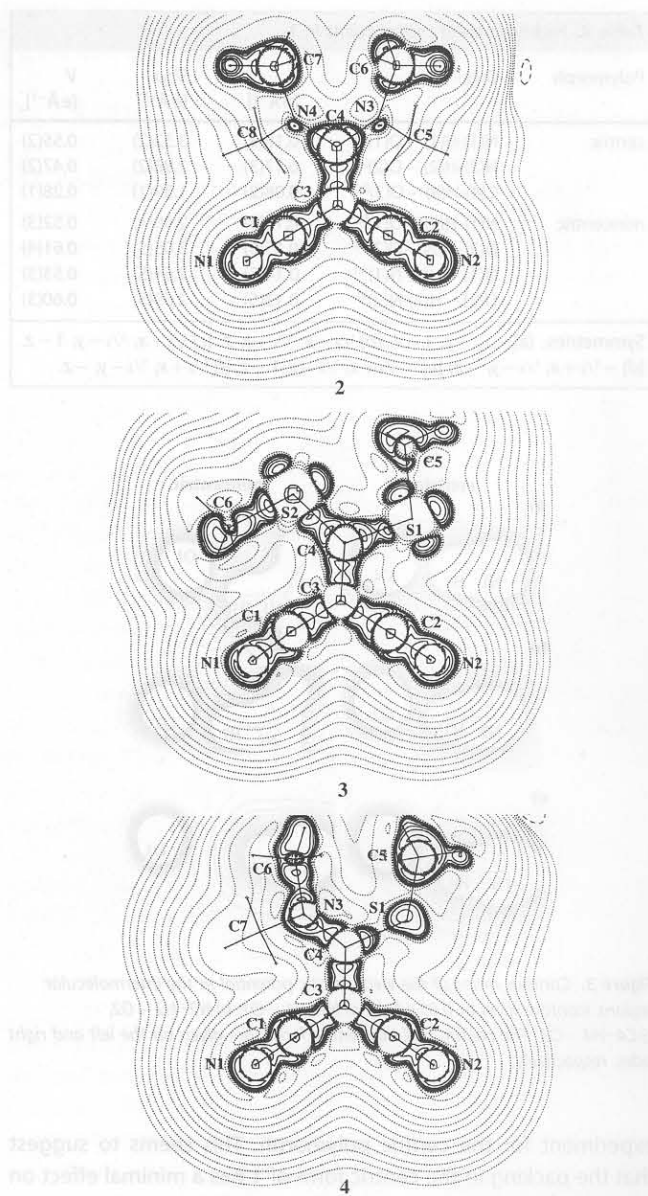


Figure 6. Contour maps of the Laplacian of the total electron density of the diamino **2**, dithio **3**, and thioamino **4** EDCN derivatives in the N1–C3–C4 plane.

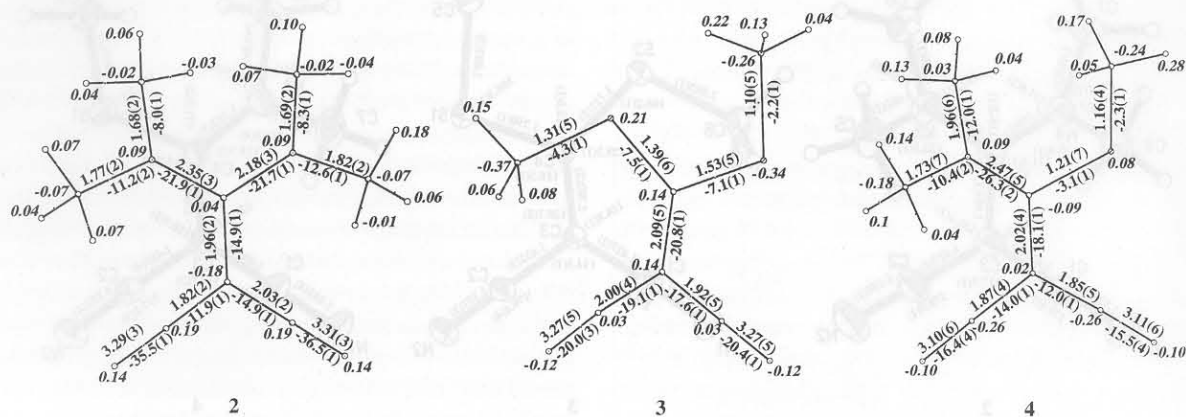


Figure 7. Stick diagrams showing the critical points for the various bonds of the diamino **2**, dithio **3**, and thioamino **4** EDCN derivatives. The electron density and the Laplacians associated with each bond are shown nearby. The pseudo-atomic charges are also indicated in italics. The atoms are labeled as in Figure 5.

case, there is probably some delocalization of electrons in the bonding region. A similar observation was made earlier by Espinosa et al.^[31] in the case of the BTDMTF-TCNQ complex. The low values of the densities and the Laplacians in the C–S bonds are characteristic of hypervalent species.^[29] A recent study on tetrasulfurtetranitride^[32] has reported low values of densities and Laplacians in the N–S bonds. The charge density analysis reflects the differences between the C_{sp^2} and C_{sp^3} bonding regions, as expected from the structural features discussed above. Accordingly, the C_{sp^2} bonding regions carry higher densities and Laplacians. Based on the pseudoatomic charges shown in Figure 7, there appears to be an increased charge separation in the noncentric thioamine 4.

The intermolecular contacts of the structures 2–4 are listed in Table 5. Both 2 and (3) exhibit five C–H...N contacts while the thioamine (4) makes only three such contacts. These are typical C–H...N contacts in terms of both the geometry and the charge density. In addition, there are intermolecular S...S and S...N contacts in the dithio compound and S...N contacts in the thioamine (Table 5). The distances as well as the charge densities associated with these contacts are similar to the contacts found in other molecules.^[29, 32]

The in situ dipole moments of the molecules in the three crystals are projected in Figure 8. The dipole moment vectors lie

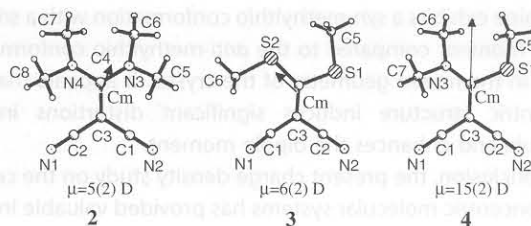


Figure 8. Molecular diagrams showing the dipole moment vectors computed from charge density in 2–4. Cm refers to the center of mass of the molecule.

close to the mean planes of the molecules. An important observation from Figure 8 is that the dipole moment of the thioamine 4, in the noncentric structure, is much higher ($\mu = 15(2)$ D) than the values of the diamino (2) and the dithio (3) derivatives in the centric structures ($\mu = 5(2)$ and $6(2)$ D).^[26] The enhancement of the dipole moment in the thioamine could arise from the asymmetric substitution of the electron donating groups or due to the noncentric crystal field. In order to shed more light, we have computed dipole moments of the three molecules in the free state in both the frozen and the optimized (AM1, PRECISE) geometries using MOPAC. In Figure 9, we depict

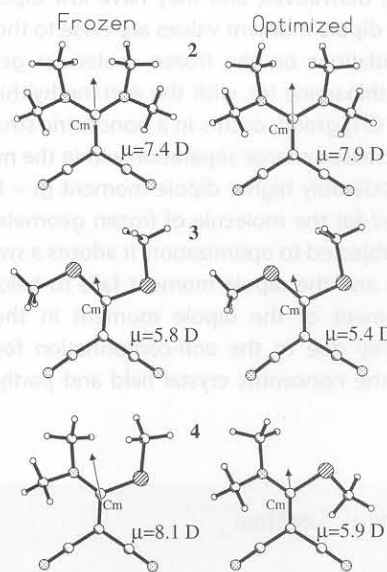


Figure 9. Molecular dipole moments calculated using AM1 (MOPAC) in the frozen (left) and the optimized (right) geometries of the diamino 2, dithio 3, and thioamino 4 EDCN derivatives. Cm refers to the center of mass of the molecule. Atomic labeling is given in Figure 8.

the frozen and the optimized dipole moments projected along with the molecule. The calculated dipole moment remains essentially unchanged between the frozen and the optimized geometries in the case of 2 and 3. Compared to the in-crystal dipole moment, these values are slightly higher in the diamino and are comparable in the case of the dithio compound (see Figures 8 and 9). The noncentric thioamine 4, on the other hand, exhibits much smaller dipole moments outside the lattice. Both the optimized ($\mu = 5.9$ D) and the frozen ($\mu = 8.1$ D) moments are considerably lower than the in-crystal dipole moment of $\mu = 15$ D. It is interesting that in the optimized geometry, the

Table 5. Intermolecular contacts in 2–4.

Hydrogen contacts between donor (D) and acceptor (A)					
D–H...A	H...A	D...A	\angle D–H...A	ρ	$\nabla^2\rho$
	[Å]	[Å]	[°]	[e Å ⁻³]	[e Å ⁻⁵]
2					
C5–H5A...N1 ^[a]	2.745	3.531	130.9	0.061(3)	0.601(2)
C7–H7A...N1 ^[b]	2.510	3.467	149.6	0.103(5)	0.967(2)
C8–H8C...N1 ^[c]	2.872	3.649	130.4	0.041(2)	0.41(1)
C8–H8B...N2 ^[d]	2.720	3.353	137.2	0.059(3)	0.616(1)
C7–H7B...N2 ^[e]	2.493	3.504	136.8	0.103(5)	0.951(2)
3					
C6–H6C...N1 ^[f]	2.564	3.541	152.8	0.035(6)	0.653(5)
C6–H6A...N1 ^[g]	2.840	3.500	120.6	0.042(5)	0.523(3)
C5–H5B...N1 ^[h]	2.586	3.631	168.6	0.04(2)	0.619(5)
C5–H5A...N2 ^[i]	2.560	3.603	167.8	0.040(2)	0.522(2)
C6–H6A...N2 ^[j]	2.886	3.554	121.3	0.048(4)	0.566(3)
4					
C5–H5B...N1 ^[k]	2.594	3.617	162.0	0.032(8)	0.572(9)
C6–H6B...N1 ^[k]	2.780	3.633	137.5	0.025(8)	0.420(4)
C5–H5A...N2 ^[l]	2.443	3.463	161.2	0.05(1)	0.691(4)
Sulfur contacts					
	Distance	ρ	$\nabla^2\rho$		
	[Å]	[e Å ⁻³]	[e Å ⁻⁵]		
3					
S1...S1 ^[m]	3.515	0.067(1)	0.654(2)		
S1...S1 ^[n]	3.952	0.030(1)	0.305(1)		
N2...S2 ^[o]	3.307	0.055(1)	0.603(1)		
N2...S2 ^[p]	3.549	0.055(1)	0.603(1)		
4					
N1...S1 ^[q]	3.194	0.055(2)	0.586(3)		
Symmetries: [a] $x, -1/2+y, 1/2+z$. [b] $3/2-x, -1/2+y, -z$. [c] $1/2+x, 3/2-y, z$. [d] $2-x, 3/2-y, -1/2+z$. [e] $3/2-x, y, -1/2+z$. [f] $1+x, y, z$. [g] $-x, 1-y, -z$. [h] $-1/2-x, 1/2+y, 1/2-z$. [i] $1-x, 1-y, 1-z$. [j] $1/2-x, 1/2+y, 1/2-z$. [k] $2-x, -y, 1/2+z$. [l] $2-x, 1-y, 1/2+z$. [m] $1-x, 1-y, 1-z$. [n] $-x, 1-y, 1-z$. [o] $1/2-x, -1/2+y, 1/2-z$. [p] $-1/2-x, -1/2+y, 1/2-z$. [q] $3/2-x, -1/2+y, -1/2+z$.					

thioamine exhibits a *syn*-methylthio conformation with a smaller dipole moment compared to the *anti*-methylthio conformation found in the frozen geometry of the crystal. It appears that the noncentric structure induces significant distortions in the molecule and enhances the dipole moment.

In conclusion, the present charge density study on the centric and noncentric molecular systems has provided valuable insight into the effect of the crystal field on molecular properties. In the case of 5-nitouracil, the dipole moment is 5.5(6) D in the centric structure and increases to 9(1) D in the noncentric lattice, while the molecular geometry essentially remains the same; the difference in the dipole moments clearly arises from the crystal packing. In the centric structure, there are N–H...O hydrogen bonded dimers, whereas in the noncentric the molecules form N–H...O linear chains. The centric crystal exhibits an additional contact, C–H...O_{nitro}, absent in the noncentric structure. The molecular dipole moment in the noncentric crystal is considerably greater than the value calculated for a free molecule of outside the crystal (frozen geometry). In centric polymorph, the dipole moment is close to that obtained from the free molecule.

In the ethylenedicarbonitriles, the crystal is centrosymmetric when the two substituents are the same, as in the diamino (**2**) and dithio (**3**) derivatives, and they have low dipole moments ($\mu \sim 6$ D). The dipole moment values are close to those obtained by AM1 calculations on the frozen molecular geometries. In contrast, the thioamine (**4**), with the *anti*-methylthio conformation of the S–CH₃ group, occurs in a noncentric structure where there is an increased charge separation within the molecule and, hence, a considerably higher dipole moment ($\mu = 15(2)$ D) than that calculated for the molecule of frozen geometry. When the molecule is subjected to optimization, it adopts a *syn*-methylthio conformation and the dipole moment falls to below $\mu = 5.9$ D. The enhancement of the dipole moment in the thioamino system is partly due to the *anti*-conformation forced on the molecule by the noncentric crystal field and partly due to the field itself.

Experimental Section

On cooling an aqueous solution of 5-nitouracil from 70 °C, crystals of the centrosymmetric polymorph were obtained. The noncentric crystals were obtained from an acetonitrile solution at room temperature. The dinitriles **2–4** were synthesized by employing reported procedures^[33–35] and the crystals were grown from toluene, ethyl acetate, and benzene solutions, respectively. High quality crystals were chosen after examination under an optical microscope. X-ray diffraction intensities were measured by ω scans using a Siemens three-circle diffractometer.

The unit cell parameters and the orientation matrix of the crystal were initially determined using ~ 45 reflections from 25 frames collected over a small ω scan of 7.5° sliced at 0.3° intervals. A hemisphere of reciprocal space was then collected in two shells using the SMART software^[36] with 2θ at 28° and 70°. Data reduction was performed using the SAINT program^[36] and the orientation matrix along with the detector and the cell parameters were refined for every 40 frames. Further experimental details are listed in Table 1. The crystal structures were first determined with the low-resolution

data up to $(\sin \theta)/\lambda = 0.56 \text{ \AA}^{-1}$. The phase problem was solved by direct methods and the non-hydrogen atoms were refined anisotropically, by means of the full-matrix least-squares procedures using the SHELXTL program.^[37] All the hydrogen atoms were located using the difference Fourier method and the temperature factors of these atoms were refined isotropically. The crystal structures agreed well with those reported previously.^[27, 38, 39] The structure of the centrosymmetric 5-nitouracil polymorph (*Pbca*) is reported for the first time and deposited in the Cambridge Crystallographic Database.

Charge density analysis was carried out based on multipole expansion of the electron density centered at the nucleus of the atom.^[40] Accordingly, the aspherical atomic density can be described in terms of spherical harmonics [Eq. (2)]. Thus, for each atom, in which the origin at the atomic nucleus, [Eq. (3)] holds. The population coefficients, P_{imp} , are to be refined along with the κ and κ' parameters which control the radial dependence of the valence shell density. The analysis was carried out in several steps.

$$\rho_{\text{atom}}(r) = \rho_{\text{core}}(r) + \rho_{\text{valence}}(r) + \rho_{\text{def}}(r) \quad (2)$$

$$\rho_{\text{atom}}(r) = \rho_{\text{core}}(r) + P_v \kappa^3 \rho_{\text{valence}}(\kappa r) + \sum_{l=0}^{\infty} \kappa'^3 R_l(\kappa' \zeta r) \sum_{m=0}^l \sum_{p=\pm l} P_{\text{imp}} Y_{\text{imp}}(\theta, \varphi) \quad (3)$$

The hydrogen atomic positions were found using the difference Fourier method and were adjusted to average neutron values,^[41] as is usually done during the multipole refinement ($C_{\text{sp}^2}\text{-H}$ 1.06, $C_{\text{sp}^3}\text{-H}$ 1.083, N–H 1.01 Å). A high order refinement of the data was performed using reflections with $(\sin \theta)/\lambda \geq 0.6 \text{ \AA}^{-1}$ and $F_0 \geq 4\sigma$. All the hydrogen atoms were held constant throughout the refinement along with their isotropic temperature factors. Multipolar refinement for the charge density analysis was carried out using the XDLSM routine of the XD package;^[42] details are given in Table 1. The atomic coordinates and the thermal parameters obtained from the high order refinement were used as input to XD refinement. Sulphur atoms were refined up to hexadecapole moments, carbon, nitrogen, and oxygen atoms up to octapole moments, while hydrogen atoms were restricted to dipole moments. During the refinement, the charge neutrality constraint was applied in all the cases. Kappa refinement was carried out on both the spherical and deformation valence shells of the non-hydrogen atoms, while those for the hydrogen atoms were restricted to the spherical valence. The multipolar refinement strategy was the following: a) scale factor, b) P_v , c) P_{imp} , d) repeat (b, c) until convergence, e) κ , f) repeat (b, c) until convergence, g) κ' , h) repeat (b, c) until convergence, i) positional and thermal parameters of all nonhydrogen atoms, and finally j) P_v and P_{imp} together. The quality of the refinement was monitored using the residual density; the magnitude of the highest residual peak in the final refinement was 0.19, 0.2, 0.2, 0.2, 0.15 e Å⁻³ for the centric **1**, noncentric **1**, **2**, **3**, and **4**, respectively. Difference mean-square displacement amplitudes for the various bonds obtained from XD were found to follow closely the Hirshfeld criterion.^[43]

The XDPROP routine was used to calculate the total electron density $\rho(r)$, the Laplacian $\nabla^2\rho$, and the ellipticity ϵ , at the bond critical points (CPs). Electrostatic potential (V) and dipole moments were also obtained using this routine. The Laplacian maps have been plotted using the XDGRAPH routine. The MOPAC program^[44] was used for the calculation of the dipole moments at the frozen and optimized molecular geometries. This calculation, although semiempirical, is known to provide reliable estimates of molecular dipole moments.^[16]

[1] P. N. Prasad, J. D. Williams, *Introduction to Nonlinear Optical Effects in Molecules and Polymers*, Wiley, New York, 1990.

[2] J. Zyss, *Molecular Nonlinear Optics: Materials, Physics, Devices*, Academic Press, Boston, 1994.

- [3] C. Bosshard, K. Sutter, P. Pretre, J. Hullinger, M. Florsheimer, P. Kaatz, P. Gunter, *Organic Nonlinear Optical Materials*, Gordon & Breach, Amsterdam, **1995**.
- [4] D. S. Chemla, J. Zyss, *Nonlinear Optical Properties of Organic Molecules and Crystals*, Academic Press, Orlando, FL, **1987**.
- [5] D. R. Kanis, M. A. Ratner, T. J. Marks, *Chem. Rev.* **1994**, *94*, 195.
- [6] E. Espinosa, C. Lecomte, E. Molins, S. Veintemillas, A. Cousson, W. Paulus, *Acta Crystallogr. Sect. B* **1996**, *52*, 519.
- [7] A. Puig-Molina, A. Alvarez-Larena, J. F. Piniella, S. T. Howard, F. Baert, *Struct. Chem.* **1998**, *9*, 395.
- [8] S. T. Howard, M. B. Hursthouse, C. W. Lehmann, P. R. Mallinson, C. S. Frampton, *J. Chem. Phys.* **1992**, *97*, 5616.
- [9] C. Gatti, V. R. Saunders, C. Roetti, *J. Chem. Phys.* **1994**, *101*, 10686.
- [10] A. Fkyerat, A. Guelzim, F. Baert, W. Paulus, G. Heger, J. Zyss, A. Perigaud, *Acta Crystallogr. Sect. B* **1995**, *51*, 197.
- [11] A. Fkyerat, A. Guelzim, F. Baert, J. Zyss, A. Perigaud, *Phys. Rev. B* **1996**, *53*, 16236.
- [12] N. K. Hansen, J. Protas, G. Marnier, *C. R. Acad. Sci. Ser. B* **1988**, *307*, 475.
- [13] N. K. Hansen, J. Protas, G. Marnier, *Acta Crystallogr. Sect. B*, **1991**, *47*, 660.
- [14] M. A. Spackman, *Annu. Rep. Prog. Chem. Sect. C* **1998**, *94*, 177.
- [15] P. Coppens in *X-ray Charge Densities and Chemical Bonding*, Oxford University Press, **1997**.
- [16] F. Hamazaoui, F. Baert, J. Zyss, *J. Mater. Chem.* **1996**, *6*, 1123.
- [17] G. K. H. Madsen, F. C. Krebs, B. Lebeck, F. K. Larsen, *Chem. Eur. J.* **2000**, *6*, 1797.
- [18] H. Youping, S. Genbo, W. Bochang, J. Rihong, *J. Cryst. Growth* **1992**, *119*, 393.
- [19] M. C. Etter, *Acc. Chem. Res.* **1990**, *23*, 120.
- [20] P. R. Mallinson, K. Wozniak, T. Garry, K. L. McCormack, *J. Am. Chem. Soc.* **1997**, *119*, 11 502.
- [21] P. R. Mallinson, K. Wozniak, C. C. Wilson, K. L. McCormack, D. M. Yufit, *J. Am. Chem. Soc.* **1999**, *121*, 4640.
- [22] W. T. Klooster, S. Swaminathan, R. Nanni, B. M. Craven, *Acta Crystallogr. Sect. B* **1992**, *48*, 217.
- [23] R. F. Stewart in *The Application of Charge Density Research to Chemistry and Drug Design* (Eds.: G. A. Jeffrey, J. F. Piniella), Plenum, New York, **1991**.
- [24] R. F. W. Bader, *Atoms in Molecules—A Quantum Theory*, Clarendon Press, Oxford, **1990**.
- [25] R. Srinivasa Gopalan, G. U. Kulkarni, S. Renganayaki, E. Subramanian, *J. Mol. Struct.* **2000**, *524*, 169.
- [26] Following referee comments, R_{int} for centric **1** and **4** were improved to ~ 0.04 by eliminating reflections above 0.9 \AA^{-1} . The dipole moments did not vary significantly.
- [27] H. U. Hummel, H. Procher, *Acta Crystallogr. Sect. C* **1986**, *42*, 1602.
- [28] N. U. Kamath, K. Venkatesan, *Acta Crystallogr. Sect. C* **1984**, *40*, 1211.
- [29] K. L. McCormack, P. R. Mallinson, B. C. Webster, D. S. Yufit, *J. Chem. Soc. Faraday Trans.* **1996**, *92*, 1709.
- [30] D. Cremer, E. Kraka, *Croat. Chem. Acta.* **1984**, *57*, 1259.
- [31] E. Espinosa, E. Molins, C. Lecomte, *Phys. Rev. B* **1997**, *57*, 1820.
- [32] W. Scherer, M. Spiegler, B. Pedersen, M. Tafipolsky, W. Hieringer, B. Reinhard, A. J. Downs, G. S. McGrady, *Chem. Commun.* **2000**, 635.
- [33] E. Ericsson, J. Sandström, I. Wennerbeck, *Acta Chem. Scand.* **1970**, *24*, 3102.
- [34] L. Dalgaard, H.-K. Andersen, S.-O. Lawesson, *Tetrahedron* **1973**, *29*, 2077.
- [35] N. H. Nilsson, *Synthesis* **1974**, 433.
- [36] Siemens Analytical X-ray Instruments, **1995**, Madison, WI, USA.
- [37] SHELXTL (SGI version), Siemens Analytical X-ray Instruments, **1995**, Madison, WI, USA.
- [38] J. G. Bergman, G. R. Crane, B. F. Levine, C. G. Bethea, *Appl. Phys. Lett.* **1972**, *20*, 21.
- [39] D. Adhikesavulu, K. Venkatesan, *Acta Crystallogr. Sect. C* **1983**, *39*, 589.
- [40] N. K. Hansen, P. Coppens, *Acta Crystallogr. Sect. A* **1978**, *34*, 909.
- [41] F. H. Allen, O. Kennard, D. G. Watson, L. Brammer, A. G. Orpen, R. Taylor, *J. Chem. Soc. Perkin Trans. 2* **1987**, S1.
- [42] T. Koritsansky, S. T. Howard, T. Richter, P. R. Mallinson, Z. Su, N. K. Hansen, *XD, A Computer Program Package for Multipole Refinement and Analysis of Charge Densities from Diffraction Data*, Cardiff University (UK), **1995**.
- [43] H. L. Hirshfeld, *Acta Crystallogr. Sect. A* **1976**, *32*, 239.
- [44] J. J. P. Stewart, *J. Comput. Aided Mol. Des.* **1990**, *4*, 1.

Received: June 26, 2000 [Z57]